

Article

Integrative Transcriptomics and Proteomics Elucidate the Regulatory Mechanism of *Hydrangea macrophylla* Flower-Color Changes Induced by Exogenous Aluminum

Haixia Chen , Denghui Wang , Yali Zhu , Wenfang Li , Jiren Chen  and Yufan Li 

Hunan Mid-Subtropical Quality Plant Breeding and Utilization Engineering Technology Research Center, College of Horticulture, Hunan Agricultural University, Changsha 410128, China; yaocyfancywz@stu.hunau.edu.cn (D.W.); 986zhuyali@stu.hunau.edu.cn (Y.Z.); liwenfang@stu.hunau.edu.cn (W.L.); chenjiren@hunau.edu.cn (J.C.); liyufan@hunau.edu.cn (Y.L.)

* Correspondence: chenhaixia@hunau.edu.cn

Abstract: The mechanism through which *Hydrangea macrophylla* are able to change color has been the focus of investigation for many studies. However, the molecular mechanism involved in the complexation of aluminum ions and anthocyanins to regulate the color change remains unclear. Here, the color-changing mechanism was investigated in *Hydrangea macrophylla* plants under aluminum stress using proteome and transcriptome sequencing methods. Catalase, peroxidase, superoxide dismutase, 3-O-delphinidin and Al³⁺ contents in sepal were significantly upregulated upon Al³⁺ treatment. Moreover, 1628 differentially expressed genes and 448 differentially expressed proteins were identified between the treated and untreated conditions. GO and KEGG enrichment analyses revealed that the differentially expressed genes and differentially expressed proteins were enriched in categories related to the cell wall, peroxidase activity, and peroxisome pathways. Importantly, eight genes involved in anthocyanin biosynthesis were significantly downregulated at the transcript and protein levels under aluminum stress. These results suggest that aluminum ions induce expression changes of related key genes, which regulate the hydrangea's flower color. Overall, this study provides a valuable reference for the molecular mechanism relating to the color change and adaptation of *Hydrangea macrophylla* in response to aluminum stress.

Keywords: *Hydrangea*; exogenous aluminum; anthocyanin; transcriptome; proteome



Citation: Chen, H.; Wang, D.; Zhu, Y.; Li, W.; Chen, J.; Li, Y. Integrative Transcriptomics and Proteomics Elucidate the Regulatory Mechanism of *Hydrangea macrophylla* Flower-Color Changes Induced by Exogenous Aluminum. *Agronomy* **2022**, *12*, 969. <https://doi.org/10.3390/agronomy12040969>

Academic Editor: Carmine Guarino

Received: 16 March 2022

Accepted: 15 April 2022

Published: 17 April 2022

Publisher's Note: MDPI stays neutral with regard to jurisdictional claims in published maps and institutional affiliations.



Copyright: © 2022 by the authors. Licensee MDPI, Basel, Switzerland. This article is an open access article distributed under the terms and conditions of the Creative Commons Attribution (CC BY) license (<https://creativecommons.org/licenses/by/4.0/>).

1. Introduction

Aluminum is the most abundant metallic element in the Earth's crust, accounting for approximately 7% of the total planet's mass. Large quantities of aluminum easily dissolve in acidic soil, which produces a bio toxic aluminum cation Al³⁺ [1]. Different plants possess alternative mechanisms to resist aluminum toxicity, some of which include an external exclusion, such as a cell wall fixation of aluminum [2], the induced establishment of a rhizosphere pH barrier [3], organic acid and aluminum complexation [4], internal tolerance theories, such as the intracellular organic-acid chelation of aluminum, vacuole partition isolation [5], aluminum-induced protein synthesis [6], and formation of induced aluminum-resistant enzyme systems [7]. Aluminum has been shown to increase peroxidase activity, enhance plasma-membrane integrity, decrease lignification, and delay aging in the tea plant, which potentially explains how aluminum promotes growth [8]. Therefore, the effect of aluminum stress on plants is a complex physiological and biochemical process.

Hydrangea macrophylla is an important ornamental plant of the *Hydrangea* genus and is popular for its large inflorescence and rich color. The inflorescence is composed of a small number of fertile flowers and a large number of sterile flowers, while the ornamental part represents the calyx of the sterile flowers [9]. *Hydrangea macrophylla* also constitute aluminum-accumulating plants. Thus, they were chosen as the primary model in which

to analyze the aluminum tolerance mechanisms [10,11]. Throughout the cultivation of *Hydrangea macrophylla*, the regulation of the flower color is the most complex process because it involves the regulation of soil pH, metal ions, and light levels alongside several other factors. Indeed, the *Hydrangea macrophylla* generates pink flowers in neutral or alkaline soils, and blue in acidic soil [12]. Numerous studies have demonstrated that aluminum is an important factor in the *Hydrangea macrophylla* flowers color alteration. The addition of aluminum ions into the soil promotes a tendency in all varieties of *Hydrangea macrophylla* to turn blue, alongside significantly increasing the plant's anthocyanin content. Only the calyx, among these varieties, can easily undergo discoloration changes from red to blue or purple [13]. Ito et al. discovered that in *Hydrangea macrophylla* varieties that co-produce red and blue petals, the Al^{3+} level was 40 times higher in the blue-petal than in the red-petalled cells [14]. Furthermore, Schreiber et al. analyzed the pigment and Al^{3+} content in several red, purple, and blue *Hydrangea macrophylla* cultivars. Schreiber and co-authors identified that the Al^{3+} contents in the petals of the red, purple, and blue cultivars were 0–10 $\mu\text{g/g}$ FW (fresh weight), 10–40 $\mu\text{g/g}$ FW, and >40 $\mu\text{g/g}$ FW, respectively [15]. Since Al^{3+} and delphinidin-3-glucoside form a complex that generates the color-related reactions, these observations suggest that the variation in coloration relates to differences in their levels.

Flower color is an important characteristic of ornamental plants, and its consistent improvement is an important aim during breeding. Anthocyanin is a water-soluble flavonoid pigment that accumulates in vacuoles and ultimately produces the plant's colors [16,17]. Previous studies investigating the mechanism underlying the color change in *Hydrangea macrophylla* have recently confirmed that changes in aluminum and anthocyanin levels are important factors in the *Hydrangea macrophylla* turning blue. However, few studies have analyzed the specific molecular mechanism related to the changes in the *hydrangea macrophylla* genes, and specifically the identification of key genes, which cause the *hydrangea macrophylla* to turn blue under aluminum stress. Therefore, this study aimed to evaluate this mechanism using proteomic and transcriptomic sequencing to provide a molecular basis for the modulation of the *Hydrangea macrophylla* flower color.

2. Materials and Methods

2.1. Plant Growth and Sampling

Hydrangea macrophylla cultivars 'Rosy Mother' were used as material. Prior to use, they were cultivated in a greenhouse (daytime, approximately 25 °C; nighttime, >5 °C) within the Nursery Garden of the Hunan Agricultural University. The cuttings were planted and transplanted into 10 cm pots filled with soil in 2017, and transplanted into 24 cm pots in February 2019. The *Hydrangea macrophylla* flower buds were grown to approximately 2 cm. After which, 10 pots of the *Hydrangea macrophylla* plants were treated with 1000 mL of a 50 $\mu\text{mol/L}$ AlCl_3 solution (containing 0.5 $\mu\text{mol/L}$ CaCl_2 , pH 4.5), and 10 pots were treated with 1000 mL of a normal water solution (containing 0.5 $\mu\text{mol/L}$ CaCl_2 , pH 4.5). The treatments were performed 1 time per 7 days, and a total of 5 times were imposed. Each treatment was repeated three times. Following the complete coloration of the sepal, one was randomly selected from any of the 10 plants and stored at -80 °C prior to physiological assays, or proteome and transcriptome analyses.

2.2. Enzyme-Activity Assays

Superoxide dismutase (SOD, EC 1.15.1.1), peroxidase (POD, EC 1.11.1.7), and catalase (CAT, EC 1.11.1.6) activities alongside the soluble protein content were all quantitated using commercial kits (Nanjing Jiancheng Bioengineering Institute, Nanjing, China). Using a cold mortar and pestle in an ice bath, fresh calyx samples (0.1 g) were thoroughly ground into a 4 mL 0.9% (*w/v*) normal saline solution that contained homogenizing glass beads. The homogenate was centrifuged at 2500 rpm for 10 min at 4 °C. The supernatant (herein referred to as the crude extract) was used for the quantitation. The absorbance of each reaction mixture was assessed using a spectrophotometer (UV-1780, Shimadzu, Japan). To

quantitate the soluble protein content, the crude extract was first vortexed and incubated at 60 °C for 30 min, before spectrophotometric assessment occurred at an absorbance of 562 nm. Since 50% hydroxylamine inhibition occurs at 37 °C, the SOD activity was quantitated at 550 nm and expressed as units per mg of total protein. The POD activity was quantitated at 420 nm and denoted in units per mg of protein such that one unit represents 1 µg guaiacol per minute at 37 °C. Finally, the CAT activity was quantitated by a decrease in absorbance at 405 nm and calculated in units per mg of total protein, whereby one unit represents 1 µmol H₂O₂ consumption per second at 37 °C.

2.3. RNA Extraction

Total RNA was extracted using Trizol Reagent (Invitrogen, Carlsbad, USA) as per the manufacturer's procedure. The RNA quantity and purity were analyzed using a Bioanalyzer 2100 and the RNA 1000 Nano LabChip Kit (Agilent, Santa Clara, USA). Importantly, all the RNA samples possessed an RIN number > 7.0. The poly(A)-tailed RNA in 5 µg total RNA was extracted twice using magnetic beads attached to a poly-T. Afterward, the poly(A)-tailed RNA was fragmented using divalent cations at an elevated temperature. Subsequently, the cleaved RNA fragments were reverse-transcribed to generate a cDNA library using an mRNA-Seq Sample Preparation Kit (Illumina, San Diego, CA, USA) according to the manufacturer's instructions. The average insert size of each paired-end library was 300 bp (±50 bp). Paired-end sequencing was performed in an IlluminaHiSeq4000 by LC Sciences, USA. Each treatment was repeated three times.

2.4. De Novo Assembly, Unigene Annotation, and Functional Classification

Cut adapt [18] and in-house Perl scripts were used to remove the contaminated reads containing adaptor sequences, or low-quality/undetermined bases. The sequence quality was verified using FastQC (<http://www.bioinformatics.babraham.ac.uk/projects/fastqc/>) (accessed on 1 June 2020) and included the Q20, Q30, and GC-content of the clean data. All the downstream analyses were based on high-quality clean data. De novo assembly of the transcriptome was performed using Trinity 2.4.0 [19]. The Trinity group transcripts formed clusters according to the shared sequence content. Here, a "gene" is used to very loosely denote a transcript cluster. The longest transcript in the cluster was chosen as the "gene" sequence (a.k.a. Unigene).

The assembled Unigenes were aligned against the non-redundant (nr) protein database (<http://www.ncbi.nlm.nih.gov/>) (accessed on 19 August 2020), in addition to the Gene Ontology (GO) (<http://www.geneontology.org>) (accessed on 19 August 2020), SwissProt (<http://www.expasy.ch/sprot/>) (accessed on 19 August 2020), Kyoto Encyclopedia of Genes and Genomes (KEGG) (<http://www.genome.jp/kegg/>) (accessed on 19 August 2020), and eggNOG (<http://eggnogdb.embl.de/>) (accessed on 19 August 2020) databases, by using DIAMOND [20] with an *E*-value threshold of $<1 \times 10^{-5}$.

2.5. Differentially Expressed Unigenes

Salmon [21] was used to assess the expression levels of the Unigenes by calculating the TPM [22]. The differentially expressed Unigenes presenting a log₂ (fold change) >1 or <−1, alongside statistical significance (*p*-value < 0.05) were identified using the 'edgeR' R package [23].

2.6. Proteome Analyses

Method S-1 provides information regarding the sample preparation, SDS-PAGE separation, FASP digestion, HPLC and LC-MS/MS analyses, data analyses, Gene Ontology annotation, KEGG pathway annotation, and functional enrichment analysis.

2.7. Quantitative Reverse Transcription–Polymerase Chain Reaction (qRT-PCR)

qRT-PCR was conducted in accordance with the method previously described by Osorio et al. [24]. Three replicates were performed for each sample. The primers used are

listed in Table S1. The relative gene expression levels were normalized using the $2^{-\Delta\Delta CT}$ method [25].

2.8. Data Analysis

The experimental results were expressed as mean \pm standard error and analyzed using Excel 2010 and SPSS 22.0. Statistical significance among the different data sets was determined using Duncan's multiple range test. A p -value < 0.05 was considered statistically significant.

2.9. Accession Numbers

The RNA-Seq data are available at the SRA-Archive (<http://www.ncbi.nlm.nih.gov/sra>) (accessed on 29 November 2021) under the accession number PRJNA785340.

The mass-spectrometry proteomics data were deposited in the ProteomeXchange Consortium (<https://www.ebi.ac.uk/pride/archive/>) (accessed on 3 December 2021) via the PRIDE partner repository with the dataset identifier PXD030168. Username: reviewer_pxd030168@ebi.ac.uk. Password: z0MsUoUz.

3. Results

3.1. Phenotypic and Biochemical Responses of *Hydrangea macrophylla* to Different Al^{3+} Conditions

Initial phenotypic investigations revealed that under normal conditions the *Hydrangea macrophylla* exhibits a red color (CK), while Al^{3+} stress promoted it to turn blue (Figure 1A,B). Subsequent quantification of the sepals' 3-O-delphinidin and Al^{3+} contents in *Hydrangea macrophylla* under Al^{3+} stress identified that both were significantly increased by 50.00% and 147.73%, respectively, compared to baseline CK levels ($p < 0.05$) (Figure 1C). Additionally, antioxidant enzyme activities in *Hydrangea macrophylla* were also significantly altered under Al^{3+} stress; namely, the activities of CAT, POD, and SOD increased by 57.95%, 170.58%, and 73.30%, respectively, compared to CK levels ($p < 0.05$).

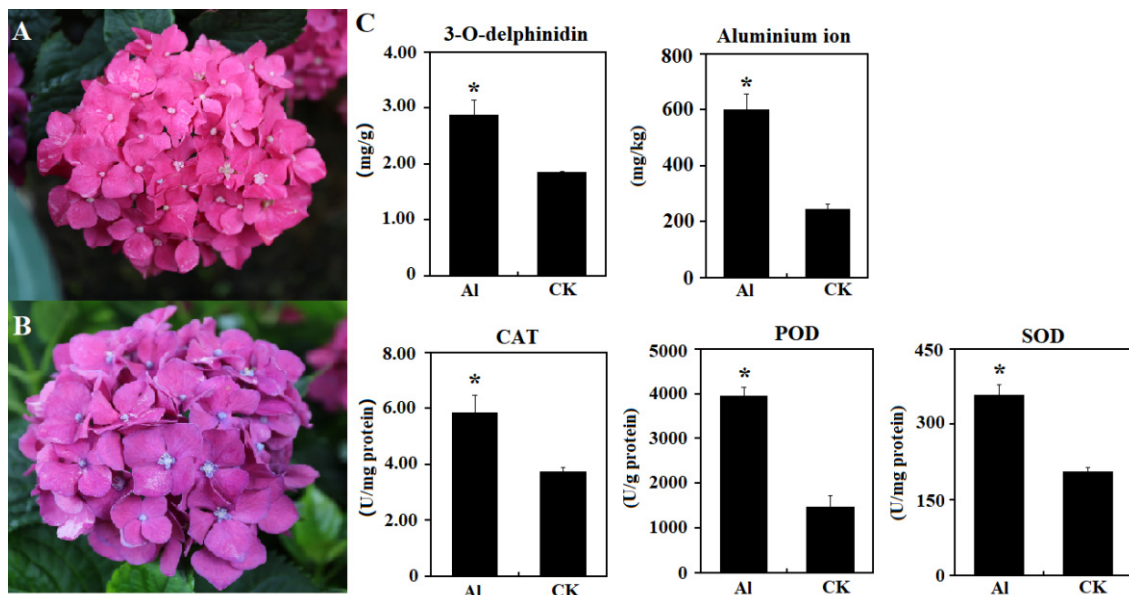


Figure 1. Phenotypic and biochemical responses to aluminum stress by *Hydrangea macrophylla*. *Hydrangea macrophylla* under normal conditions (A) and Al^{3+} stress (B). The asterisk (*) represents a significant difference between normal conditions and Al^{3+} stress ($p < 0.05$).

3.2. Differential Proteomic and Transcriptomic Profiles Result from Varying Al³⁺ Conditions

IlluminaHiseq4000 sequencing eliminated the joints and low-quality sequences and produced 300,312,550 clean high-quality reads and 41.91 Gb of transcriptomic data from the six samples. The Q30 bases ranged between 93.18% and 93.37%, while the GC average content was approximately 44.88%. De novo assembly of the sequenced reads by Trinity identified 58,989 genes, of which 58,396 were quantified (Table S2; see also Supplemental Information—Table S2). A total of 56,124 genes were quantified from both the Al³⁺ stress and CK conditions, while 548 and 1724 genes were quantified only in the Al³⁺ stress and CK conditions, respectively (Figure 2A).

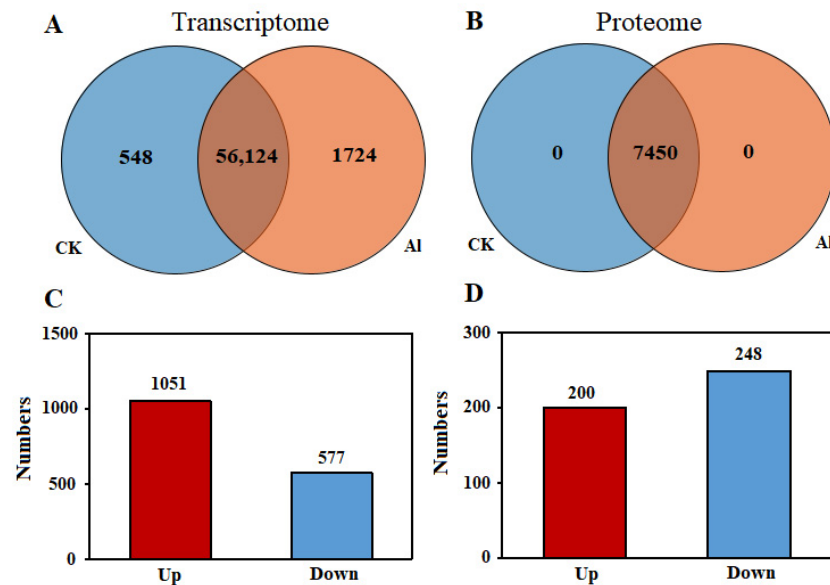


Figure 2. A statistical representation of the quantified transcripts and proteins. Venn diagrams for the quantified transcripts (A) and proteins (B) under Al³⁺ treatment (red) or CK (blue). The amounts of differentially expressed genes (C) and proteins (D).

Based on the chosen criteria for peptide and protein identification, 49,419 (96.82%) of the 51,043 peptides were identified as unique peptides (FDR ≤ 0.01) (Table S3; see also Supplemental Information—Table S3). A total of 8007 proteins (FDR ≤ 0.01) were identified, and 7450 proteins (93.04%) were quantified based on these peptides (Table S4; see also Supplemental Information—Table S4). Finally, these 7450 proteins were quantified for both the Al³⁺ stress and CK conditions (Figure 2B).

3.3. Identification of Differentially Expressed Genes (DEGs) and Proteins (DEPs)

There were 1628 DEGs and 448 DEPs identified in the Al³⁺-treated group compared to the CK. Within the 1628 DEGs, 1051 genes were upregulated, and 577 was downregulated, meaning the number of upregulated genes were significantly higher than those downregulated (Figure 2C). Conversely, the expression of DEPs illustrated the opposite pattern, whereby 200 proteins were upregulated and 248 were downregulated in the Al³⁺-treated group compared to the CK. Thus, the number of downregulated proteins was significantly higher than those upregulated (Figure 2D).

Further analysis of the DEGs revealed that the known Al³⁺ stress genes: *PIN-LIKES like 1* (*PIN1*, TRINITY_DN23911_c0_g3), *PIN-LIKES like 3* (*PIN3*, TRINITY_DN16208_c0_g1), and *probable auxin efflux carrier component 1c* (*PIN1A*, TRINITY_DN18284_c3_g2), were all significantly downregulated upon Al³⁺ treatment. Likewise, protein expression of *PIN1* and *PIN3* was also significantly downregulated under the Al³⁺ stress, yet there was no significant difference in *PIN1A* protein levels. Moreover, there was no significant difference in the transcript levels of auxin influx carrier (*AUX1*, TRINITY_DN18969_c0_g5), although the protein level significantly decreased following Al³⁺-treatment.

3.4. GO Analyses of the DEGs and DEPs

To elucidate any functional differences, the DEGs and DEPs were analyzed for GO enrichment based on the clustering analysis (Figure 3). The largest groups identified in the DEGs and DEPs relating to biological processes were in “translation” and the “oxidation-reduction process”, respectively. Furthermore, “nucleus” and “plasma membrane” were the predominant molecular-function elements exhibited in the DEGs and DEPs, respectively. The “structural constituent of the ribosome” and “protein-binding” were the predominant cellular components that belonged to these DEGs and DEPs, respectively. Both the DEGs and DEPs were enriched in the “cell wall organization”, “cell wall”, and “plant cell wall” categories, although the functional classifications displayed many differences in the enrichment of the DEGs and DEPs.

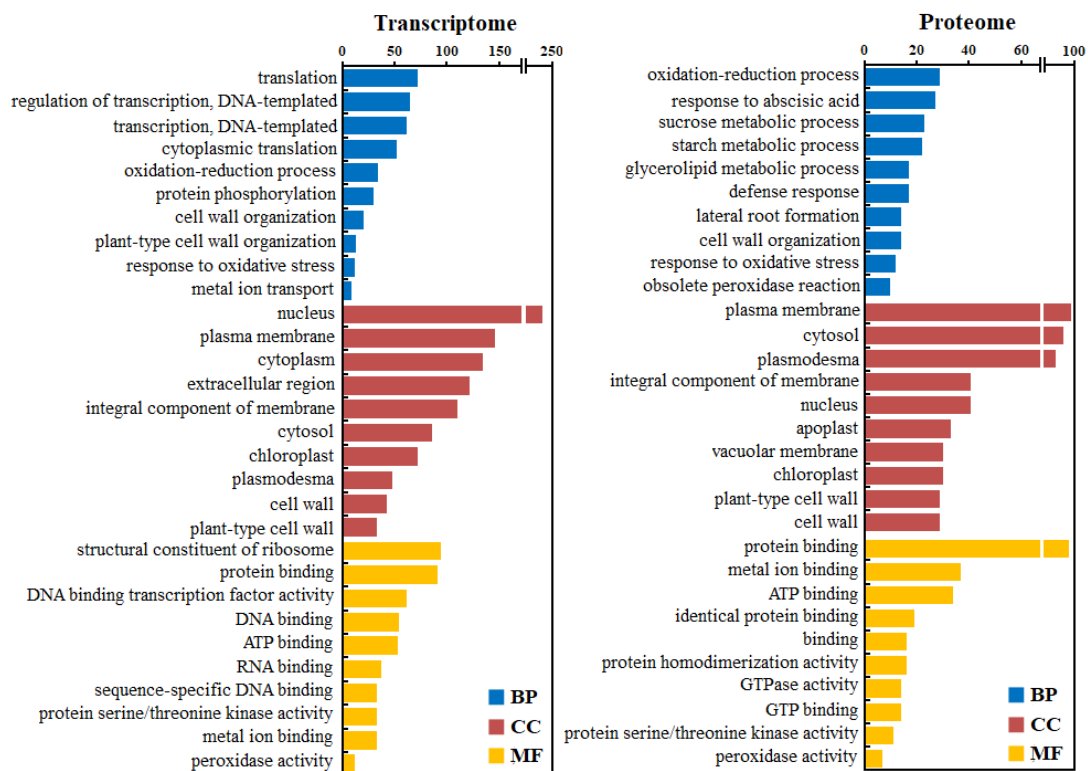


Figure 3. GO analyses of the differentially expressed genes and proteins. BP: Biological process; MF: Molecular function; CC: Cellular component.

The DEPs relating to “cell wall synthesis” were selected for further analysis (Figure 4). The protein levels of most of the related proteins showed no significant changes under aluminum stress, however, the probable pectin esterase/pectin esterase inhibitor 34 (TRINITY_DN21120_c1_g1) and xyloglucan galactosyltransferase (TRINITY_DN18508_c3_g3) were both significantly downregulated by 1.16- and 1.01-fold, respectively. The levels of putative pectin esterase/pectin esterase inhibitor (TRINITY_DN21120_c0_g1 and TRINITY_DN21120_c1_g1), pectin acetyl esterase 8 (TRINITY_DN23590_c2_g2), and cell wall synthesis-related proteins (TRINITY_DN20393_c0_g2, TRINITY_DN23875_c1_g2, and TRINITY_DN21527_c1_g1) were significantly decreased compared to the control levels. Conversely, the levels of chitinase (TRINITY_DN18332_c0_g6) and end chitinase EP3 (TRINITY_DN20209_c0_g1) were significantly increased. Meanwhile, the protein levels of three heat-shock proteins (TRINITY_DN14670_c0_g1, TRINITY_DN18453_c3_g1, and TRINITY_DN19474_c0_g1) related to cell wall synthesis were similarly found to be significantly increased under the Al³⁺ stress. This observation suggests that these proteins play an important role in regulating the cell wall structure of the petals during Al³⁺ stress.

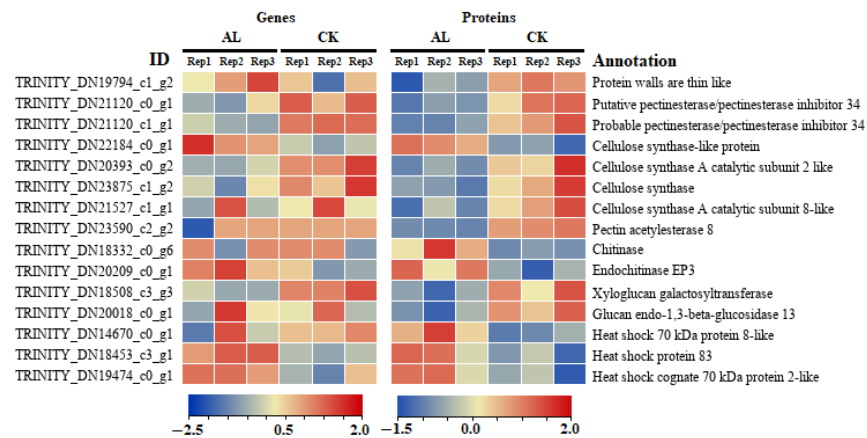


Figure 4. Heat-map analyses of the differentially expressed proteins related to cell wall synthesis.

3.5. KEGG Analyses of the DEGs and DEPs

KEGG pathway analyses were performed to reveal the functions of the DEGs/DEPs that might be related to the Al^{3+} stress response. Pathway annotation results showed that 1628 DEGs and 449 DEPs were classified into 109 and 214 pathways, respectively. It was found that the DEGs were primarily enriched in the ribosome (106) (Figure 5). The DEPs were principally enriched in the metabolic pathways (80), followed by involvement in the biosynthesis of secondary metabolites (46) (Figure 5). Interestingly, many DEGs and DEPs were discovered to both be enriched in the peroxisome pathway. These results suggest that genes involved in the peroxisome pathway are connected to the *Hydrangea macrophylla* response to Al^{3+} stress.

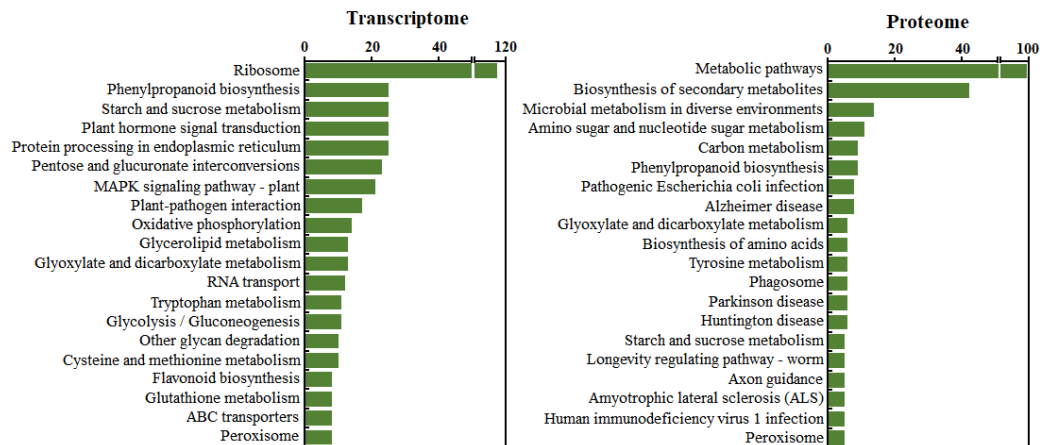


Figure 5. KEGG pathway analyses of the differentially expressed genes and proteins.

3.6. Differential Expression Analysis of Antioxidation-Related Genes at the Transcript and Protein Levels

The GO analysis demonstrated DEG and DEP enrichment of peroxidase-activity categories, alongside the KEGG pathway analysis revealed enrichment of the peroxisome, which implies that antioxidation-related proteins could play an important role in the Al^{3+} stress-related change in flower color. Therefore, these changes in the differentially expressed antioxidation-related protein levels were selected for further analysis. The expression levels of 10 antioxidant proteins (eight peroxidases and two catalases) were shown to significantly change under Al^{3+} stress (Figure 6A). Peroxidases can be divided into soluble peroxidases and cell wall-bound peroxidases. Here, peroxidase 7 (TRINITY_DN17819_c1_g4), peroxidase 4-like (TRINITY_DN19022_c1_g1), and peroxidase 4 (TRINITY_DN21867_c1_g6) were found to both be enriched in peroxidase activity categories and also significantly enriched in plant-type cell wall categories. These data indicate that these proteins can play

a role against oxidative stress in addition to participating in the cell wall synthesis and its structural regulation. Among these DEPs, peroxidase 4, lignin-forming anionic peroxidase (TRINITY_DN21720_c1_g4), and peroxisomal catalase-like (TRINITY_DN8646_c0_g1) were significantly upregulated under Al^{3+} stress. Additionally, the majority of these DEPs were significantly upregulated under aluminum stress compared with the control levels. The only exceptions being peroxidase 43 (TRINITY_DN20035_c1_g6) and peroxisomal catalase (TRINITY_DN20002_c3_g7).

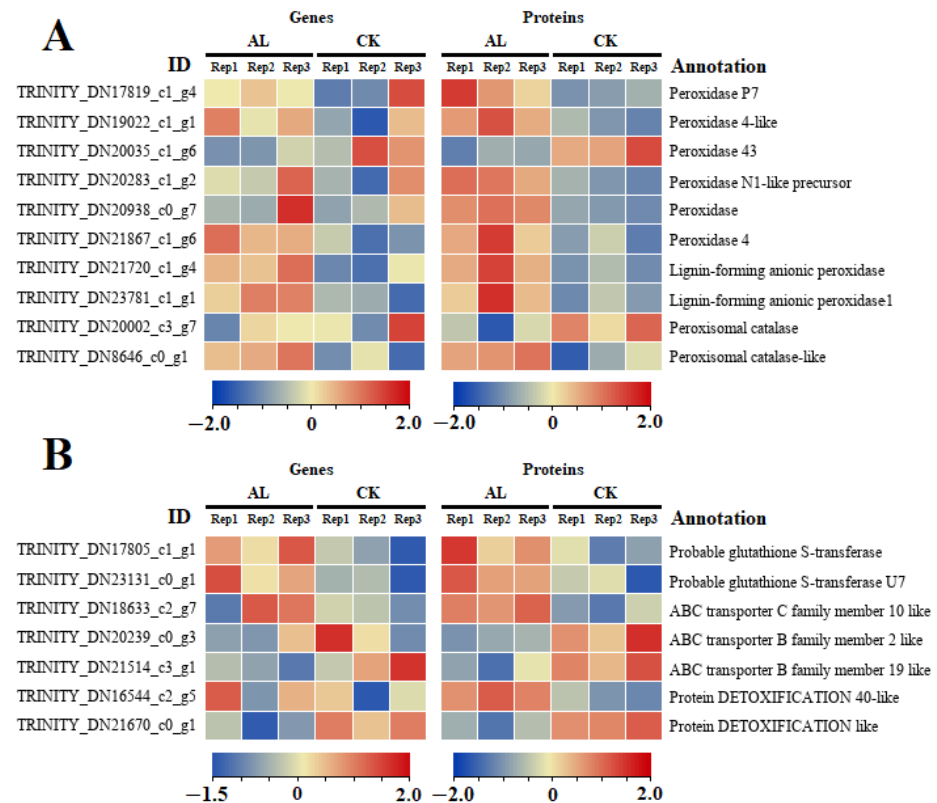


Figure 6. Heat-map analysis of the differentially expressed proteins involved in antioxidation (A) and anthocyanin transport (B).

3.7. Differential Expression Analysis of Anthocyanin Transporters

Anthocyanin transporters are important proteins that regulate anthocyanins. Here, seven DEPs related to anthocyanin transport were identified, including two glutathione S-transferase proteins (GSTs), three ATP-binding cassette (ABC) transporter proteins, and two detoxification (DTX) proteins (Figure 6B). Within these groups of differentially expressed proteins, two glutathione s-transferases (GST, TRINITY_DN17805_c1_g1 and GST U7, TRINITY_DN23131_c0_g1), one ABC transporter C family member 10-like (ABCC10, TRINITY_DN18633_c2_g7), and one detoxification protein (DTX 40, TRINITY_DN16544_c2_g5) were significantly upregulated following Al^{3+} stress. Conversely, three DEPs, including ABCB2 (TRINITY_DN20239_c0_g3), ABCB19 (TRINITY_DN21514_c3_g1), and DTX24 (TRINITY_DN21670_c0_g1) were significantly downregulated under Al^{3+} stress. The transcript level of only the GST gene was significantly upregulated compared with the corresponding CK level, which correlated to the change in protein level. Additionally, the expressions of *ABCB19* and *DTX24* were significantly downregulated, whereas no significant changes were illustrated in the other four genes.

3.8. Differential Expression Analysis of the Genes Involved in the Anthocyanin Metabolic Pathway

The expression levels of genes related to the anthocyanin biosynthesis pathway were also significantly affected by the Al^{3+} treatment at the transcript and protein levels. The results showed that eight genes related to the anthocyanin biosynthesis pathway were significantly downregulated under Al^{3+} stress compared with the CK levels (Figure 7). These included the transcript levels of chalcone synthase (*CHS*, TRINITY_DN20366_c1_g6) and flavonol synthase (*FLS*, TRINITY_DN20628_c0_g9), which decreased significantly compared with the CK levels. However, the protein levels showed no significant changes. The transcript levels of the chalcone isomerase (*CHI*, TRINITY_DN16945_c0_g1), anthocyanidin 3-O-glucosyltransferase (*BZ1*, TRINITY_DN17786_c1_g6), and *F3',5'H* (TRINITY_DN15745_c0_g3) genes did not significantly alter under Al^{3+} stress, yet there was a significant decrease in their protein levels. Moreover, both the transcript and protein levels of flavanone 3-hydroxylase (*F3H*, TRINITY_DN22725_c2_g5) and dihydroflavonol 4-reductase (*DFR*, TRINITY_DN18805_c2_g2) decreased significantly under Al^{3+} stress.

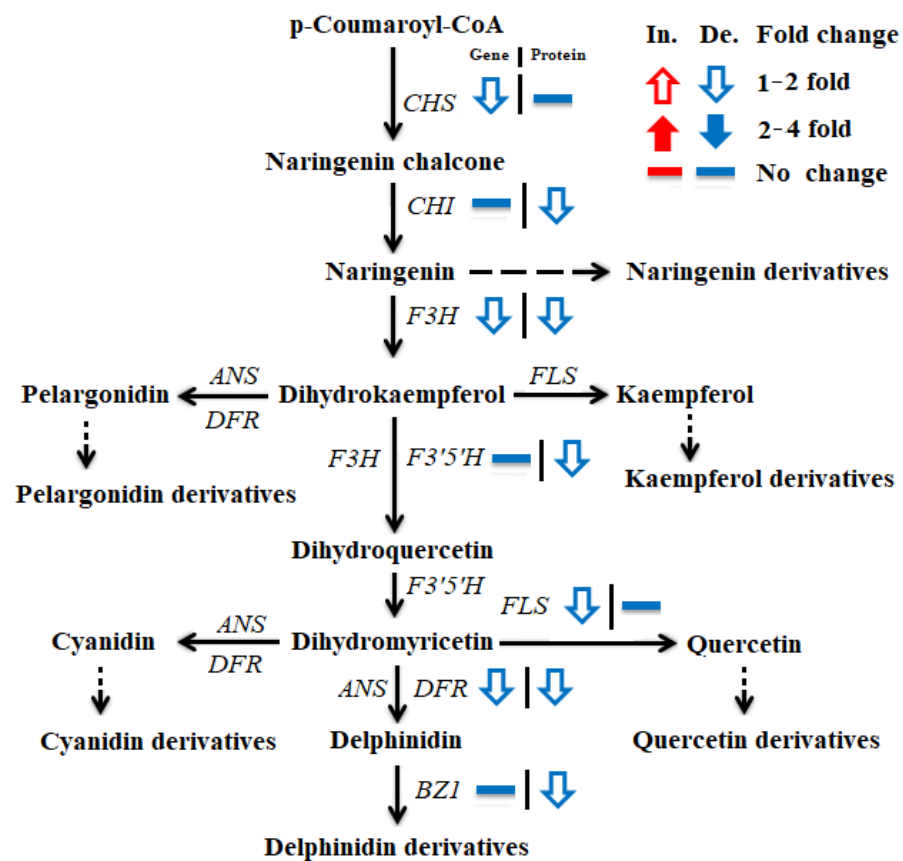


Figure 7. Comparative analysis between the aluminum-stressed and normal conditions of the expression levels for genes involved in the anthocyanin biosynthesis pathway.

3.9. qRT-PCR Validation of the Gene Expression Patterns

To validate the RNA-Seq results, qRT-PCR analysis was performed on 12 genes (*PIN3*, *PIN1*, *PEI34*, *XLT2*, *FLS*, *AOP1*, *Ligin forming anionic POD*, *GST*, *Peroxisomal CAT*, *DFR*, *ABC19*, and *DTX24*) using gene-specific primers. The results demonstrated similar trends to the RNA-Seq data (Figure 8), thus confirming the reliability of the TPM values for each transcript that was previously determined by the RNA-Seq.

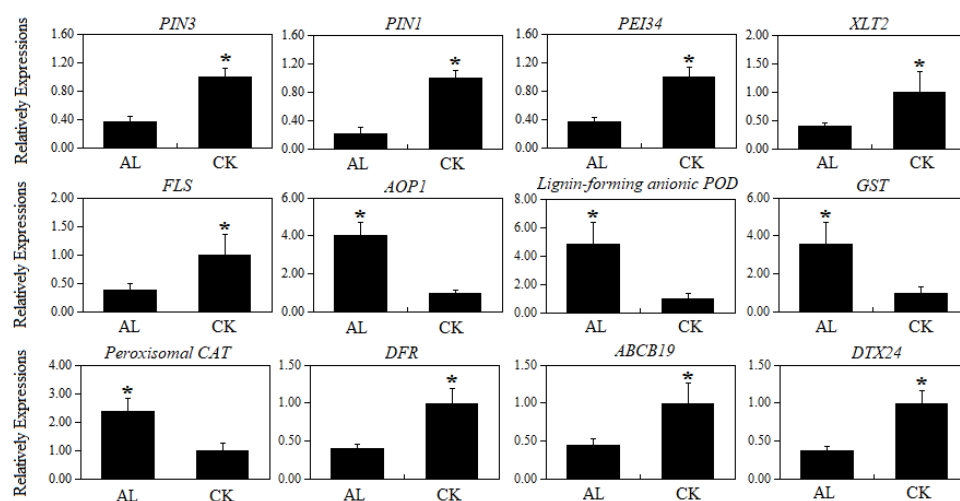


Figure 8. qRT-PCR-based expression analyses of representative genes that are differentially expressed according to the RNA-Seq results ($p < 0.05$). The asterisk (*) represents a significant difference between normal conditions and Al^{3+} stress.

4. Discussion

Interestingly, the cell wall has a fixation effect on aluminum during plant growth. The plant's cell walls are negatively charged and thus can complex with cations [26], while components such as polysaccharides and proteins located in cell walls can combine with aluminum [27]. Consequently, the cell wall acts as the first barrier against aluminum in plants. The various components contained within it, such as glue and cellulose, can bind to the aluminum on the cell surface and reduce the amount of cellular aluminum intake [28]. *Panax notoginseng* can grow under high concentrations of aluminum since the pectin component in the root cell wall binds to approximately 64–75% of the aluminum [29]. A mechanism exists that causes the pectin levels in the cell wall to change in response to the plant undergoing aluminum stress. Therefore, changes in cell wall composition play a role in altering the aluminum level and cell wall tolerance to aluminum. The levels of cellulose and pectin in the cell wall are regulated by cellulose synthase and pectin methyltransferase. Studies have shown that the activity of pectin methyltransferase is low in aluminum-tolerant varieties under aluminum stress, resulting in a high degree of pectin methylation. Subsequently, promoting a reduction in the cell wall levels net negative charge and suppression of Al^{3+} binding to the cell wall [30]. In this study, the PME34 (TRINITY_DN21120_c0_g1, TRINITY_DN21120_c1_g1) protein abundance decreased significantly under aluminum stress. This result indicates that pectin methyltransferase activity similarly decreased following aluminum treatment, resulting in an increase in pectin methylation and a reduction in the accumulation and binding of Al^{3+} ions in the cell wall. Meanwhile, the level of cellulose synthase-like protein (TRINITY_DN22184_c0_g1) in the cell wall was significantly increased. It is thus postulated that these changes in protein levels may promote the upregulation of cellulose and pectin during aluminum stress and ultimately enhance the plant's tolerance to aluminum stress.

Aluminum stress can change the accumulation and distribution of auxin; processes that are primarily regulated by AUX1 and PIN2 [31]. Indeed, both the AUX1 protein family and PIN proteins are responsible for the transportation of auxin into cells [32]. Auxin can either depend upon self-regulation or from the auxin transport carrier to participate in the aluminum tolerance process of plants. Shen et al. [33] demonstrated that aluminum stress upregulates the auxin output carrier protein, PIN2, and induces its accumulation at the cell membrane, which damages the polar transport of auxin. This observation suggests that the auxin transport protein may directly bind to aluminum and transport it to cells through the auxin intracellular transport pathway. Therefore, any aluminum originally bound to the cell wall or cell membrane may be transported into cells through endocytosis [34]. In this

study, the AUX1 (TRINITY_DN18969_c0_g5), PIN1 (TRINITY_DN23911_c0_g3), and PIN3 (TRINITY_DN16208_c0_g1) proteins were significantly downregulated under aluminum stress, possibly through the inhibition of PIN and AUX1 protein expression in the petals following extended aluminum stress. This observation is consistent with previous results in *Arabidopsis* root-tip cells [35], in which either short-term aluminum treatment or a low aluminum concentration significantly upregulated the PIN2 protein. Contrastingly, either long-term aluminum treatment or a high aluminum concentration downregulated PIN2 protein expression.

Plants under stress activate their own defense systems to protect their ability to continue growing. Aluminum toxicity enhances the activities of antioxidant enzymes, which enables plants to more thoroughly remove excess reactive oxygen species and further enhance aluminum tolerance [36]. Indeed, aluminum-tolerant wheat and rice can enhance antioxidant-enzyme activity or upregulate non-enzyme antioxidants in root tips to comprehensively remove reactive oxygen species and increase their aluminum tolerance. Moreover, overexpression of alternate oxidases enhances the aluminum tolerance of tobacco [37]. Tamas et al. [38] illustrated that aluminum-induced inhibition of root elongation positively correlates with aluminum-induced peroxidase activity. Furthermore, the root peroxidase activity of sensitive cultivars under aluminum stress is significantly higher than in tolerant cultivars. Many crops show increased peroxidase activity in roots under aluminum stress [39,40]. Additionally, peroxidase has two functions: It can provide an antioxidant effect and it can also participate in the cell wall cross-linking process [41,42]. Consequently, the activities of the antioxidant enzymes POD, CAT, and SOD in *Hydrangea macrophylla* were significantly increased, in this study, under aluminum stress. Moreover, peroxidase 7, peroxidase 4, and peroxidase 4-like, which are involved in the cell wall synthesis, and peroxidase and catalase, which play antioxidant roles, were also significantly upregulated. These results showed that peroxidase-related enzymes enhance the aluminum stress tolerance of *Hydrangea macrophylla* by regulating the antioxidant capacity and cell wall cross-linking.

Recent studies indicate that transcriptional regulation of stress tolerance genes plays an important role in aluminum tolerance [43]. MATE is a family of detoxification transporters and Sivaguru et al. [44] have previously shown that aluminum can induce SbMATE gene expression through the accumulation of reactive oxygen species. Additionally, Sivaguru and co-authors revealed that SbMATE expression levels are positively correlated with the secretion rate of citric acid. The GsMATE protein in *Arabidopsis* uses aluminum to induce the citrate transporter and is potentially involved in the regulation of its sensitivity to aluminum toxicity [45]. Therefore, previous studies have concluded that the MATE expression levels in crops are positively correlated with the aluminum tolerance of these plants [46]. Meanwhile, studies have shown that when rice roots are exposed to aluminum stress, OsSTAR1 forms a complex with OsSTAR2 and functions in the role of an ABC transporter. UDP-glucan is transported to the cell wall to reduce the number of aluminum binding sites there, thus providing the plant with aluminum resistance [47]. Overall, these results suggest that ABC transporters can confer resistance to aluminum stress. Indeed, Negishi et al. [48] have found that two genes encoding ABC transporters, *HmVALT* and *HmPALT*, are involved in the aluminum tolerance mechanism within blue *Hydrangea macrophylla* sepals. Correspondingly, DETOXIFICATION 40-like (TRINITY_DN16544_c2_g5) and ABCC10 were significantly upregulated in this study under aluminum stress. Furthermore, this change may enhance the resistance of *Hydrangea macrophyllas* to aluminum stress. Genetic and biochemical evidence suggests that the MATE and ABC transporters can both resist aluminum stress and also participate in the transmembrane transport of anthocyanins from the cytoplasm to the vacuoles [49,50]. Zhao et al. [51] presented that *MtMATE2* located in vacuoles preferentially transported anthocyanin malonate and that it was stably expressed in anthocyanin-rich *Arabidopsis* stem and leaf cells. Glutathione s-transferase (GST) plays an auxiliary role in anthocyanin transfer from the endoplasmic reticulum to the vacuoles [52,53]. Presently, several anthocyanin-related GSTFs have been identified in

various plants. For example, TT19 [54], VvGST1 [55], LcGST4 [56], and GhGSTF2 [57] are all involved in both anthocyanin accumulation and synthesis. This study also established that two GST proteins are significantly upregulated under aluminum stress, which is consistent with previous studies, suggesting that GST proteins are also involved with anthocyanin metabolism in the *Hydrangea macrophylla*.

The genes in the anthocyanin metabolism pathway regulate the levels and proportions of anthocyanin metabolites. Delphinidin is considered to be the most common and main anthocyanin in blue flowers [58]. Nakamura et al. inhibited the expression of the CHS gene in blue gentian and subsequently obtained white gentian. Alternatively, inhibition of the ANS gene expression in blue petunia promoted the petals to change color to a light blue [59]. The F3H and F3',5'H genes encode the red cyanidin and blue delphinium pigments, respectively, and represent key genes in determining the anthocyanin species. These genes belong to cytochrome P450 monooxygenase [60], which catalyzes the hydroxylation of the flavonoid B ring at the 3'- and 3' 5'- sites. They compete with the substrate dihydrokaempferol (DHK), which determines the final product of flavonoids and is an important enzyme in determining color formation [61]. High expression of F3',5'H coupled with low expression of F3H can effectively give rise to blue flowers following domination by the delphinidin pigment [62]. However, F3H, F3',5'H, CHS, CHI, FLS, DFR, and BZ1 were all found to be downregulated in this study, whereas the delphinidin content was significantly upregulated compared to the control levels. This observation may be due to the long-term aluminum stress, which can cause significant downregulation of proteins related to the anthocyanin pathway. However, the absence of any toxic effect at the early stages of aluminum stress prompted a large number of delphinidins to accumulate. Concurrently, Al³⁺ can react with phenolic hydroxyl and methoxyl groups in anthocyanin molecules to generate blue chelates, which are not easily degraded [63]. Notably, the proteins related to the anthocyanin synthesis pathway were downregulated in the later stages of aluminum stress. However, the decomposition rate of anthocyanin still remained lower than the downregulated synthesis rate, which ultimately resulted in the accumulation of delphinidins, meaning the blue flower color of the *Hydrangea macrophylla* was maintained.

5. Conclusions

Exogenous aluminum stress significantly increases the 3-O-delphinidin levels and the activities of catalase, peroxidase, and superoxide dismutase. Additionally, the expression levels of genes related to the cell wall, peroxidase activity, and peroxisome pathways are affected. Under aluminum stress, the auxin transport carrier proteins PIN1, PIN3, and AUX1, alongside cell wall-synthesis-related proteins, PMI34 and CES, are significantly downregulated. Conversely, antioxidase proteins, such as the lignin-forming anionic, POD and POD4, peroxisomal CAT, the anthocyanin transporters, GST and DTX40, in addition to the ABC transporters, ABCB2 and ABCB19, are significantly upregulated. The differential expression of these proteins enhances the adaptability to aluminum stress and promotes the synthesis of 3-O-delphinidin. Additionally, genes related to anthocyanin biosynthesis are significantly downregulated under aluminum stress. Accordingly, this study provides a valuable reference for the molecular mechanism related to the color change and adaptation of *Hydrangea macrophylla* in response to aluminum stress.

Supplementary Materials: The following are available online at <https://www.mdpi.com/article/10.3390/agronomy12040969/s1>, Table S1: Quantitative identification of ERFs, Table S2: Number of metabolites identified, Table S3: The first thirty differential metabolites of $|\log_2fc| > 2$ in each comparison group, Table S4: Correlation analysis of the top 100 differential metabolites and the top 50 differential genes in *p*-value ranking.

Author Contributions: Conceived and designed the experiments: H.C. Per-formed the experiments: H.C., D.W., Y.Z. and W.L. Analyzed the data: J.C., Y.L. and D.W. Contributed reagents/materials/analysis tools: H.C., J.C. and Y.L. Wrote the paper: H.C. All authors have read and agreed to the published version of the manuscript.

Funding: This work was funded by a project of the Natural Science Foundation of Hunan (2021JJ30313).

Institutional Review Board Statement: Not applicable.

Informed Consent Statement: Not applicable.

Data Availability Statement: The RNA-Seq data generated in this study are available at the SRA-Archive (<http://www.ncbi.nlm.nih.gov/sra>) (accessed on 29 November 2021) with accession number PRJNA785340.

Conflicts of Interest: The authors declare no conflict of interest.

References

1. Von Uexküll, H.R.; Mutert, E. Global extent, development and economic impact of acid soils. *Plant Soil* **1995**, *171*, 1–15. [[CrossRef](#)]
2. Kochian, L.V.; Piñeros, M.A.; Hoekenga, O.A. The Physiology, Genetics and Molecular Biology of Plant Aluminum Resistance and Toxicity. *Plant Soil* **2005**, *274*, 175–195. [[CrossRef](#)]
3. Yang, Z.-B.; Rao, I.M.; Horst, W.J. Interaction of aluminium and drought stress on root growth and crop yield on acid soils. *Plant Soil* **2013**, *372*, 3–25. [[CrossRef](#)]
4. Ma, J.F.; Hiradate, S. Form of aluminium for uptake and translocation in buckwheat (*Fagopyrum esculentum* Moench). *Planta* **2000**, *211*, 355–360. [[CrossRef](#)]
5. Zhang, F.; Yan, X.; Han, X.; Tang, R.; Chu, M.; Yang, Y.; Yang, Y.-H.; Zhao, F.; Fu, A.; Luan, S.; et al. A Defective Vacuolar Proton Pump Enhances Aluminum Tolerance by Reducing Vacuole Sequestration of Organic Acids. *Plant Physiol.* **2019**, *181*, 743–761. [[CrossRef](#)]
6. Yang, Q.; Wang, Y.; Zhang, J.; Shi, W.; Qian, C.; Peng, X. Identification of aluminum-responsive proteins in rice roots by a proteomic approach: Cysteine synthase as a key player in Al response. *Proteomics* **2007**, *7*, 737–749. [[CrossRef](#)]
7. Ma, B.; Gao, L.; Zhang, H.; Cui, J.; Shen, Z. Aluminum-induced oxidative stress and changes in antioxidant defenses in the roots of rice varieties differing in Al tolerance. *Plant Cell Rep.* **2012**, *31*, 687–696. [[CrossRef](#)]
8. Ghanati, F.; Morita, A.; Yokota, H. Effects of Aluminum on the Growth of Tea Plant and Activation of Antioxidant System. *Plant Soil* **2005**, *276*, 133–141. [[CrossRef](#)]
9. Dirr, M.A. *Hydrangeas for American Gardens*; Timber Press: Portland, OR, USA, 2004.
10. Lei, Y.L.; Zhou-Qi, L.I. Tissue Culture of Stem Segment of Hydrangea macrophylla. *J. Northwest For. Univ.* **2008**, *4*, 101–103.
11. Peng, J.H.; Chen, H.X.; Gong, W.; Fu, W. Effects of aluminium stress on membrane permeability and antioxidant system in vivo Hydrangea macrophylla plants. *J. Hunan Agric. Univ.* **2013**, *39*, 42–44.
12. Anderson, N.; Weiland, J.; Pharis, J.; Gagné, W.; Janiga, E.; Rosenow, M.J. Comparative forcing of Hydrangea macrophylla ‘Bailer’ as a florist’s hydrangea. *Sci. Hortic.* **2009**, *122*, 221–226. [[CrossRef](#)]
13. Kodama, M.; Tanabe, Y.; Nakayama, M. Analyses of Coloration-related Components in Hydrangea Sepals Causing Color Variability According to Soil Conditions. *Hortic. J.* **2016**, *85*, 372–379. [[CrossRef](#)]
14. Ito, D.; Shinkai, Y.; Kato, Y.; Kondo, T.; Yoshida, K. Chemical Studies on Different Color Development in Blue- and Red-Colored Sepal Cells of Hydrangea macrophylla. *Biosci. Biotechnol. Biochem.* **2009**, *73*, 1054–1059. [[CrossRef](#)] [[PubMed](#)]
15. Schreiber, H.D.; Jones, A.H.; Lariviere, C.M.; Mayhew, K.M.; Cain, J.B. Role of aluminum in red-to-blue color changes in Hydrangea macrophylla sepals. *BioMetals* **2011**, *24*, 1005–1015. [[CrossRef](#)] [[PubMed](#)]
16. Tanaka, Y.; Sasaki, N.; Ohmiya, A. Biosynthesis of plant pigments: Anthocyanins, betalains and carotenoids. *Plant J.* **2008**, *54*, 733–749. [[CrossRef](#)] [[PubMed](#)]
17. Fukui, Y.; Tanaka, Y.; Kusumi, T.; Iwashita, T.; Nomoto, K. A rationale for the shift in colour towards blue in transgenic carnation flowers expressing the flavonoid 3',5'-hydroxylase gene. *Phytochemistry* **2003**, *63*, 15–23. [[CrossRef](#)]
18. Martin, M. Cutadapt removes adapter sequences from high-throughput sequencing reads. *EMBnet. J.* **2011**, *17*, 10–12. [[CrossRef](#)]
19. Grabherr, M.G.; Haas, B.J.; Yassour, M.; Levin, J.Z.; Thompson, D.A.; Amit, I.; Adiconis, X.; Fan, L.; Raychowdhury, R.; Zeng, Q.; et al. Full-length transcriptome assembly from RNA-Seq data without a reference genome. *Nat. Biotechnol.* **2011**, *29*, 644–652. [[CrossRef](#)]
20. Buchfink, B.; Xie, C.; Huson, D.H. Fast and sensitive protein alignment using DIAMOND. *Nat. Methods* **2015**, *12*, 59–60. [[CrossRef](#)]
21. Patro, R.; Duggal, G.; Love, M.I.; Irizarry, R.A.; Kingsford, C. Salmon provides fast and bias-aware quantification of transcript expression. *Nat. Methods* **2017**, *14*, 417–419. [[CrossRef](#)]
22. Mortazavi, A.; Williams, B.A.; McCue, K.; Schaeffer, L.; Wold, B. Mapping and quantifying mammalian transcriptomes by RNA-Seq. *Nat. Methods* **2008**, *5*, 621–628. [[CrossRef](#)] [[PubMed](#)]
23. Robinson, M.D.; McCarthy, D.J.; Smyth, G.K. EdgeR: A Bioconductor package for differential expression analysis of digital gene expression data. *Bioinformatics* **2010**, *26*, 139–140. [[CrossRef](#)] [[PubMed](#)]
24. Osorio, S.; Alba, R.; Nikoloski, Z.; Kochevenko, A.; Fernie, A.R.; Giovannoni, J.J. Integrative Comparative Analyses of Transcript and Metabolite Profiles from Pepper and Tomato Ripening and Development Stages Uncovers Species-Specific Patterns of Network Regulatory Behavior. *Plant Physiol.* **2012**, *159*, 1713–1729. [[CrossRef](#)] [[PubMed](#)]

25. Livak, K.J.; Schmittgen, T.D. Analysis of relative gene expression data using real-time quantitative PCR and the $2^{-\Delta\Delta CT}$ Method. *Methods* **2001**, *25*, 402–408. Available online: <https://www.sciencedirect.com/science/article/pii/S1046202301912629> (accessed on 8 December 2021). [[CrossRef](#)] [[PubMed](#)]
26. Liu, J.Y.; Min, Y.U.; Liu, L.P.; Xiao, H.D. Differences of Cell Wall Polysaccharides in Border Cells and Root Apices of Pea (*Pisum sativum*) Under Aluminium Stress. *Sci. Agric. Sin.* **2009**, *6*, 1963–1971.
27. Horst, W.J.; Wang, Y.; Eticha, D. The role of the root apoplast in aluminium-induced inhibition of root elongation and in aluminium resistance of plants: A review. *Ann. Bot.* **2010**, *106*, 185–197. [[CrossRef](#)]
28. Hossain, A.Z.; Koyama, H.; Hara, T. Growth and cell wall properties of two wheat cultivars differing in their sensitivity to aluminum stress. *J. Plant Physiol.* **2006**, *163*, 39–47. Available online: <https://www.sciencedirect.com/science/article/pii/S0176161705001069> (accessed on 8 December 2021). [[CrossRef](#)]
29. Ye, Y.; Chunyan, D.; Lanping, G.; Yuan, Q.; Xiaoyan, Y.; Qi, C.; Diqiu, L.; Chengxiao, W.; Xiuming, C. Distribution pattern of aluminum in *Panax notoginseng*, a native medicinal plant adapted to acidic red soils. *Plant Soil* **2017**, *423*, 375–384. [[CrossRef](#)]
30. Yang, J.L.; Li, Y.Y.; Zhang, Y.J.; Zhang, S.S.; Wu, Y.R.; Wu, P.; Zheng, S.J. Cell Wall Polysaccharides Are Specifically Involved in the Exclusion of Aluminum from the Rice Root Apex. *Plant Physiol.* **2008**, *146*, 602–611. [[CrossRef](#)]
31. Yuan, H.-M.; Liu, W.-C.; Jin, Y.; Lu, Y.-T. Role of ROS and auxin in plant response to metal-mediated stress. *Plant Signal. Behav.* **2013**, *8*, e24671. [[CrossRef](#)]
32. Teale, W.D.; Paponov, I.; Ditengou, F.A.; Palme, K. Auxin and the developing root of *Arabidopsis thaliana*. *Physiol. Plant.* **2005**, *123*, 130–138. [[CrossRef](#)]
33. Shen, H.; Hou, N.; Schlicht, M.; Wan, Y.; Mancuso, S.; Baluska, F. Aluminium toxicity targets PIN2 in *Arabidopsis* root apices: Effects on PIN2 endocytosis, vesicular recycling, and polar auxin transport. *Sci. Bull.* **2008**, *53*, 2480–2487. [[CrossRef](#)]
34. Panda, S.K.; Baluška, F.; Matsumoto, H. Aluminum stress signaling in plants. *Plant Signal. Behav.* **2009**, *4*, 592–597. [[CrossRef](#)] [[PubMed](#)]
35. Cao, H.P.; Dao-Ming, W.U.; Gan, H.H.; Shen, H. Effects of aluminum stress on the activity of PIN2 protein in *Arabidopsis thaliana* apical roots. *Guihaia* **2016**, *36*, 121–126.
36. Sharma, P.; Dubey, R.S. Involvement of oxidative stress and role of antioxidative defense system in growing rice seedlings exposed to toxic concentrations of aluminum. *Plant Cell Rep.* **2007**, *26*, 2027–2038. [[CrossRef](#)] [[PubMed](#)]
37. Panda, S.K.; Sahoo, L.; Katsuhara, M.; Matsumoto, H. Overexpression of Alternative Oxidase Gene Confers Aluminum Tolerance by Altering the Respiratory Capacity and the Response to Oxidative Stress in Tobacco Cells. *Mol. Biotechnol.* **2013**, *54*, 551–563. [[CrossRef](#)]
38. Tamás, L.; Huttová, J.; Mistrík, I. Inhibition of Al-induced root elongation and enhancement of Al-induced peroxidase activity in Al-sensitive and Al-resistant barley cultivars are positively correlated. *Plant Soil* **2003**, *250*, 193–200. Available online: <http://www.jstor.org/stable/24129946> (accessed on 12 January 2022). [[CrossRef](#)]
39. Šimonovičová, M.; Huttová, J.; Mistrík, I.; Široká, B.; Tamás, L. Root growth inhibition by aluminum is probably caused by cell death due to peroxidase-mediated hydrogen peroxide production. *Protoplasma* **2004**, *224*, 91–98. [[CrossRef](#)]
40. Achary, V.M.M.; Jena, S.; Panda, K.K.; Panda, B.B. Aluminium induced oxidative stress and DNA damage in root cells of *Allium cepa* L. *Ecotoxicol. Environ. Saf.* **2008**, *70*, 300–310. [[CrossRef](#)]
41. Passardi, F.; Penel, C.; Dunand, C. Performing the paradoxical: How plant peroxidases modify the cell wall. *Trends Plant Sci.* **2004**, *9*, 534–540. [[CrossRef](#)]
42. Passardi, F.; Cosio, C.; Penel, C.; Dunand, C. Peroxidases have more functions than a Swiss army knife. *Plant Cell Rep.* **2005**, *24*, 255–265. [[CrossRef](#)] [[PubMed](#)]
43. Kochian, L.V.; Piñeros, M.A.; Liu, J.; Magalhaes, J.V. Plant Adaptation to Acid Soils: The Molecular Basis for Crop Aluminum Resistance. *Annu. Rev. Plant Biol.* **2015**, *66*, 571–598. [[CrossRef](#)] [[PubMed](#)]
44. Sivaguru, M.; Liu, J.; Kochian, L.V. Targeted expression of SbMATE in the root distal transition zone is responsible for sorghum aluminum resistance. *Plant J.* **2013**, *76*, 297–307. [[CrossRef](#)] [[PubMed](#)]
45. Ma, Q.; Yi, R.; Li, L.; Liang, Z.; Zeng, T.; Zhang, Y.; Huang, H.; Zhang, X.; Yin, X.; Cai, Z.; et al. GsMATE encoding a multidrug and toxic compound extrusion transporter enhances aluminum tolerance in *Arabidopsis thaliana*. *BMC Plant Biol.* **2018**, *18*, 212. [[CrossRef](#)] [[PubMed](#)]
46. Liu, J.; Magalhaes, J.V.; Shaff, J.; Kochian, L.V. Aluminum-activated citrate and malate transporters from the MATE and ALMT families function independently to confer *Arabidopsis* aluminum tolerance. *Plant J.* **2009**, *57*, 389–399. [[CrossRef](#)] [[PubMed](#)]
47. Huang, C.-F.; Yamaji, N.; Mitani, N.; Yano, M.; Nagamura, Y.; Ma, J.F. A Bacterial-Type ABC Transporter Is Involved in Aluminum Tolerance in Rice. *Plant Cell* **2009**, *21*, 655–667. [[CrossRef](#)]
48. Negishi, T.; Oshima, K.; Hattori, M.; Kanai, M.; Mano, S.; Nishimura, M.; Yoshida, K. Tonoplast- and Plasma Membrane-Localized Aquaporin-Family Transporters in Blue Hydrangea Sepals of Aluminum Hyperaccumulating Plant. *PLoS ONE* **2012**, *7*, e43189. [[CrossRef](#)]
49. Debeaujon, I.; Peeters, A.J.M.; Léon-Kloosterziel, K.M.; Koornneef, M. The TRANSPARENT TESTA12 Gene of *Arabidopsis* Encodes a Multidrug Secondary Transporter-like Protein Required for Flavonoid Sequestration in Vacuoles of the Seed Coat Endothelium. *Plant Cell* **2001**, *13*, 853–871. [[CrossRef](#)]
50. Goodman, C.D.; Casati, P.; Walbot, V. A Multidrug Resistance—Associated Protein Involved in Anthocyanin Transport in *Zea mays*. *Plant Cell* **2004**, *16*, 1812–1826. [[CrossRef](#)]

51. Zhao, J.; Huhman, D.; Shadle, G.; He, X.-Z.; Sumner, L.W.; Tang, Y.; Dixon, R.A. MATE2 Mediates Vacuolar Sequestration of Flavonoid Glycosides and Glycoside Malonates in *Medicago truncatula*. *Plant Cell* **2011**, *23*, 1536–1555. [[CrossRef](#)]
52. Luo, H.; Dai, C.; Li, Y.; Feng, J.; Liu, Z.; Kang, C. Reduced Anthocyanins in Petioles codes for a GST anthocyanin transporter that is essential for the foliage and fruit coloration in strawberry. *J. Exp. Bot.* **2018**, *69*, 2595–2608. [[CrossRef](#)] [[PubMed](#)]
53. Kou, M.; Liu, Y.-J.; Li, Z.-Y.; Zhang, Y.-G.; Tang, W.; Yan, H.; Wang, X.; Chen, X.-G.; Su, Z.-X.; Arisha, M.H.; et al. A novel glutathione S-transferase gene from sweetpotato, IbGSTF4, is involved in anthocyanin sequestration. *Plant Physiol. Biochem.* **2019**, *135*, 395–403. [[CrossRef](#)] [[PubMed](#)]
54. Sun, Y.; Li, H.; Huang, J.-R. Arabidopsis TT19 Functions as a Carrier to Transport Anthocyanin from the Cytosol to Tonoplasts. *Mol. Plant* **2012**, *5*, 387–400. [[CrossRef](#)] [[PubMed](#)]
55. Conn, S.; Curtin, C.; Bézier, A.; Franco, C.; Zhang, W. Purification, molecular cloning, and characterization of glutathione S-transferases (GSTs) from pigmented *Vitis vinifera* L. cell suspension cultures as putative anthocyanin transport proteins. *J. Exp. Bot.* **2008**, *59*, 3621–3634. [[CrossRef](#)] [[PubMed](#)]
56. Hu, B.; Zhao, J.; Lai, B.; Qin, Y.; Wang, H.; Hu, G. LcGST4 is an anthocyanin-related glutathione S-transferase gene in Litchi chinensis Sonn. *Plant Cell Rep.* **2016**, *35*, 831–843. [[CrossRef](#)]
57. Li, S.; Zuo, D.; Cheng, H.; Ali, M.; Wu, C.; Ashraf, J.; Zhang, Y.; Feng, X.; Lin, Z.; Wang, Q.; et al. Glutathione S-transferases GhGSTF1 and GhGSTF2 involved in the anthocyanin accumulation in *Gossypium hirsutum* L. *Int. J. Biol. Macromol.* **2020**, *165*, 2565–2575. [[CrossRef](#)]
58. Huang, Y.Y.; Li, P.S.M.; Chen, M.C. Gene engineering of blue color flower. *Plant Physiol. Commun.* **2002**, *38*, 203–206. (In Chinese)
59. Nakamura, N.; Fukuchi-Mizutani, M.; Miyazaki, K.; Suzuki, K.; Tanaka, Y. RNAi suppression of the anthocyanidin synthase gene in *Torenia hybrida* yields white flowers with higher frequency and better stability than antisense and sense suppression. *Plant Biotechnol.* **2006**, *23*, 13–17. [[CrossRef](#)]
60. Han, Y.; Vimolmangkang, S.; Soria-Guerra, R.E.; Rosales-Mendoza, S.; Zheng, D.; Lygin, A.V.; Korban, S.S. Ectopic Expression of Apple *F3'H* Genes Contributes to Anthocyanin Accumulation in the Arabidopsis *tt7* Mutant Grown Under Nitrogen Stress. *Plant Physiol.* **2010**, *153*, 806–820. [[CrossRef](#)]
61. Wang, Y.-S.; Xu, Y.-J.; Gao, L.-P.; Yu, O.; Wang, X.-Z.; He, X.-J.; Jiang, X.-L.; Liu, Y.-J.; Xia, T. Functional analysis of Flavonoid 3',5'-hydroxylase from Tea plant (*Camellia sinensis*): Critical role in the accumulation of catechins. *BMC Plant Biol.* **2014**, *14*, 347. [[CrossRef](#)]
62. Nishihara, M.; Nakatsuka, T. Genetic engineering of flavonoid pigments to modify flower color in floricultural plants. *Biotechnol. Lett.* **2010**, *33*, 433–441. [[CrossRef](#)] [[PubMed](#)]
63. Dai, S.L.; Hong, Y. Molecular Breeding for Flower Colors Modification on Ornamental Plants Based on the Mechanism of Anthocyanins Biosynthesis and Coloration. *Sci. Agric. Sin.* **2016**, *49*, 529–542. (In Chinese)